Catalysis Letters
https://doi.org/10.1007/s10562-021-03617-5

One-Pass Conversion of Benzene and Syngas to Alkylbenzenes by Cu–ZnO–Al_2O_3 and ZSM-5 Relay

Tengfei Han[1] · Hong Xu[1] · Jianchao Liu[1] · Ligong Zhou[2] · Xuekuan Li[2] · Jinxiang Dong[1] · Hui Ge[2]

Received: 24 December 2020 / Accepted: 28 March 2021

Abstract

Alkylbenzenes have a wide range of uses and are the most demanded aromatic chemicals. The finite petroleum resources compels the development of production of alkylbenzenes by non-petroleum routes. One-pass selective conversion of benzene and syngas to alkylbenzenes is a promising alternative coal chemical engineering route, yet it still faces challenge to industrialized applications owing to low conversion of benzene and syngas. Here we presented a Cu–ZnO–Al_2O_3/ZSM-5 bifunctional catalyst which realizes one-pass conversion of benzene and syngas to alkylbenzenes with high efficiency. This bifunctional catalyst exhibited high benzene conversion (benzene conversion of 50.7%), CO conversion (CO conversion of 55.0%) and C7&C8 aromatics total yield (C7&C8 total yield of 45.0%). Characterizations and catalytic performance evaluations revealed that ZSM-5 with well-regulated acidity, as a vital part of this Cu–ZnO–Al_2O_3/ZSM-5 bifunctional catalyst, substantially contributed to its performance for the alkylbenzenes one-pass synthesis from benzene and syngas due to depress methanol-to-olefins (MTO) reaction. Furthermore, matching of the mass ratio of two active components in the dual-function catalyst and the temperature of methanol synthesis with benzene alkylation reactions can effectively depress the formation of unwanted by-products and guarantee the high performance of tandem reactions.

Graphic Abstract

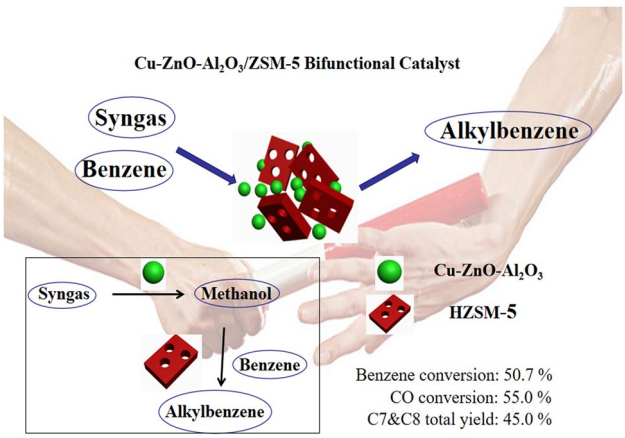

Keywords Benzene · Syngas · Alkylation · Cu–ZnO–Al_2O_3 · ZSM-5

✉ Hui Ge
gehui@sxicc.ac.cn

[1] College of Chemistry and Chemical Engineering, Taiyuan University of Technology, Taiyuan 030024, Shanxi Province, China

[2] Institute of Coal Chemistry, Chinese Academy of Sciences, Taiyuan 030001, Shanxi Province, China

1 Introduction

As important chemical intermediates, alkylbenzenes have been broadly employed in chemical industries. Such as, toluene is used as solvent, p-xylene is the main feed for the production of polyester fibers and films, o-xylene and

Published online: 13 May 2021

meta-xylene can be used for production of plasticizers, pesticides, dyes, and medicine intermediates [1, 2]. At present, catalytic reforming technology of petroleum refinery is the dominant method for production of alkylbenzenes. However, the crude resources are depleted increasingly. In 2020, the COVID-19 epidemic swept the world [3, 4], adding uncertainty to the international economy environment and affecting the supply chain of petroleum industry. Hence there is necessary to develop non-petroleum routes for the production of alkylbenzenes. It is widely accepted that coal is one of the most abundant and widely distributed conventional energy, but the disadvantages of coal utilization are high emission and low efficiency. Therefore, the development of coal-based technologies for the production of alkylbenzenes chemicals can not only alleviate the dependence on oil, but also can improve the efficiently use of coal resources.

At present, there are four main technical routes for obtaining alkylbenzenes from coal, namely: (1) one-step conversion of syngas to aromatics (STA) [5–8], which has the advantages of single raw material, low cost and high academic significance, but it has disadvantages such as complex products, low aromatics selectivity, and low CO effective utilization rate; (2) methanol to aromatics (MTA) [9, 10], which has the advantages of high methanol conversion rate and simple operation, but it has disadvantages such as low aromatic selectivity and poor catalyst stability; (3) alkylation of benzene with methanol to alkylbenzenes [11–14], the advantage of this technology is that the selectivity of alkylbenzenes is high, but there are disadvantages such as methanol prone to side reactions and low product yield.; and (4) alkylation of benzene with syngas to produce alkylbenzenes [15–21]. The technology of one-pass conversion of benzene and syngas to alkylbenzenes has its own unique advantages: it can eliminate the intermediate step of methanol production and the liquid products are basically aromatics, which is beneficial to the later separation and transformation. Therefore, benzene and syngas alkylation technology is preferred in industrial application. However, until now, the conversion and selectivity of benzene with syngas are still not satisfied.

Recently, the alkylation of benzene with syngas to produce alkylbenzenes has received increased attention. The catalytic system are usually composed of dual-functional components, where the precious metals or metal oxides are complexed with zeolite. The alkylation reaction of benzene and syngas is proposed as a tandem reaction. First, syngas is converted into methanol intermediates by the precious metals or metal oxides, then the generated methanol moved to zeolite, reacted with benzene forming the alkybenzenes. Among the methanol synthesis catalysts, $Cu–ZnO–Al_2O_3$ catalyst is the most widely researched and used, attributing to its low price, high activity and high selectivity. Meanwhile ZSM-5 is an important industrialized microporous zeolite. Due to its adjustable acidity, good thermal stability and unique shape-selective catalysis, ZSM-5 has been widely applied to alkylation reaction and aromatization reaction. Combining Cu based component with ZSM-5 component to catalyze the alkylation of benzene with syngas is a popular strategy. Xuebin [22] prepared $Cu\text{-}Al_2O_3$/ZSM-5 catalyst using impregnation method for the alkylation reaction of benzene with syngas. It was found that increasing the Cu content can increase the activity of the catalyst, containing 11% Cu catalyst showed the highest the 16.8% conversion of benzene at 350 °C and 1.5 MPa. They also found that the addition of a second metal (Zn, Mn or V) to the copper-based catalyst can increase the selectivity of methylation and decrease the selectivity of heavy aromatics. Gao [23] used $CuO\text{-}ZnO\text{-}Al_2O_3$/ZSM-5 bifunctional composite catalyst to catalyze the alkylation reaction of benzene and syngas in a slurry bed reactor. They modified ZSM-5 component with acid–alkali co-processing to produce meso-pores and reducing strong acid sites, which enhances mass transfer and increases aromatic selectivity.

Although the $Cu–ZnO–Al_2O_3$/ZSM-5 bifunctional catalyst has showed promising result for the tandem reaction of benzene with syngas, the lower conversion and selectivity of benzene impedes the industrial development, and it lacks the insight understanding of the coupling mechanism of methanol synthesis with benzene alkylation. Here, we presented a simple prepared $Cu–ZnO–Al_2O_3$/ZSM-5 hybrid catalyst, realizing high benzene conversion of 50.7% and high C7–C8 aromatic selectivity by the one-pass conversion of benzene and syngas to alkylbenzenes in fix-bed reactor. The matching relationship between the two active components in the bifunctional catalyst and the important role of zeolite' acidity in the alkylation reaction of benzene with syngas have been revealed. The coupling mechanism of tandem reaction was proposed.

2 Experimental

2.1 Preparation of Bifunctional Catalyst

The $Cu–ZnO–Al_2O_3$/ZSM-5 bifunctional catalysts were prepared as follows: The two components ($CuO–ZnO–Al_2O_3$ and HZSM-5) with different mass ratios were mixed and ground in a mortar for 15 min, then pressed, crushed and sieved to granules of 40–60 meshes. HZSM-5 (framework Si/Al ratio = 15, 31, 84) was obtained from Nankai University Catalyst Corp and $CuO–ZnO–Al_2O_3$ component was the commercial catalyst of Sud-Chemie company. The prepared dual-function catalysts were denoted as $Cu–ZnO–Al_2O_3$/ZSM-5 (x) = y, x represents the framework Si/Al ratio of ZSM-5 and y represents the mass ratio.

2.2 Catalyst Characterization

The HZSM-5 and CuO–ZnO–Al_2O_3 componets, as well as the hybrid catalysts, were identified using X-ray diffraction (XRD), patterns were recorded on a Rigaku Ultima IV with monochromated Cu Kα radiation at a scanning rate of 2° min^{-1} from 5° to 80°.

Solid-state magic-angle spinning nuclear magnetic resonance (MAS NMR) spectra were carried out on a Bruker Avance III 600 MHz Wide Bore spectrometer (14.4 T). The 29 Si spectra were recorded at resonance frequencies of 119.29 MHz with spinning rate of 10 kHz. The framework Si/Al ratio of ZSM-5 using the following formula, where $I_{Si(nAl)}$ represents the total area of Si(nAl) [24].

$$\frac{Si}{Al} = \sum_{n=0}^{4} I_{Si(nAl)} / \sum_{n=0}^{4} \frac{n}{4} [I_{Si(nAl)}] \quad (1)$$

The elemental composition ratio of silicon to aluminum (Si/Al) of ZSM-5 is detected by X Ray Fluorescence (XRF). The XRF was performed on a Bruker S4 Pioneer.

NH_3-TPD (temperature programmed desorption of ammonia) of the catalyst was performed on Micromeritics AutoChem II 2920. The typical test procedure was as follows: The sample was pretreated in He flow at 350 °C for 1 h and then cooled to 100 °C, then adsorption of NH_3 (40 mL/min) at 100 °C for 0.5 h. After adsorption, the sample was purged under He for 1 h. Subsequently, the temperature was raised from 100 to 800 °C at a ramping rate of 10 °C/min. The signal of NH_3 desorption was monitored by a thermal conductivity detector (TCD).

Pyridine (Py) adsorbed FT-IR studies of HZSM-5 were performed with a Bruker INVENIO R instrument. For pyridine adsorption (Py-IR), pyridine vapour was introduced into the cell at 30 °C for 1 h, after evacuation at 150 °C for 1 h to removed excess pyridine, then the spectra were recorded.

Nitrogen adsorption–desorption was carried out on a Micromeritics ASAP 2020 PLUS HD88. Before testing, all catalysts are degassed for 5 h under vacuum at 150 °C and isotherms were recorded at 77 K.

The residual sodium content of the HZSM-5 and elements ratio of CuO–ZnO–Al_2O_3 were determined by ICP-AES (inductively coupled plasma atomic emission spectroscopy) on a PerkinElmer Avio 500 instrument.

The morphology of catalysts were observed by a scanning electron microscope (SEM) on a Hitachi SU 8010.

2.3 Catalytic Reaction Tests

The alkylation reaction of benzene with syngas was carried out on a micro fixed-bed reactor of a stainless-steel tube with an inner diameter of 6 mm. Typically, 1 g catalyst (40–60 meshes) was loaded in the middle of the reaction tube and sealed by the quarts at two end. For each reaction, the flow rate of syngas ($H_2/CO = 2$) and benzene were maintained at 5220 mL/(h g_{cat}) and 2.64 g/h g_{cat} respectively. The syngas pressure was controlled at 4.0 MPa and the reaction temperature were changed between 350 and 450 °C.

Exhaust gas were analyzed by an online gas chromatographs (GC-920 from HAIXIN Chromatograph Equipment Company), which was equipped with 5 A molecular sieve packed column connected to a the thermal conductivity detector (TCD) to detect the CO and H_2, a CH_4 converter to a the flame ionization detector (FID) to analyze the CH_4, CO and CO_2, and an activated alumina column connected to another FID to detect the hydrocarbon gases. Use CH_4 established the composition correlation between FIDs and TCD, and got the composition of the exhaust gas. The condensed liquid products were collected and analyzed by an Agilent 7890 B chromatograph equipped with INNOWAX capillary column (60 mX0.32 umX0.25 nm) and FID detector. The product selectivity and conversion rate of feed were calculated on a molar carbon basis, and the calculation formulas are as follows:

$$C_B = \frac{n_{B,in} - n_{B,out}}{n_{B,in}} \times 100\% \quad (2)$$

where C_B, $n_{(B, in)}$ and $n_{(B, out)}$ represent conversion rate of benzene, mole of benzene at the inlet and outlet, respectively.

$$S_{C7} = \frac{n_{C7}}{n \sum (C7, C8, C9+)} \times 100\% \quad (3)$$

where C7, C8, C9 + represent toluene, xylene and ethylbenzene, heavy aromatics with carbon number larger than 9, $n \sum (C7, C8, C9+)$ is the total moles of liquid aromatics products., respectively. And nC7 represents mole of toluene, respectively. The calculation formula of S_{C8} and S_{C9+} refer to the above formula.

$$Y_{C7+C8} = C_B \times \left(S_{C7} + S_{C8}\right) \times 100\% \quad (4)$$

where Y_{C7+C8} represents the total yield of toluene, xylene and ethylbenzene.

$$C_{CO} = \frac{n_{CO,in} - n_{CO,out}}{n_{CO,in}} \times 100\% \quad (5)$$

where C_{CO}, $n_{(CO,in)}$ and $n_{(CO, out)}$ represent conversion rate of CO, mole of CO at the inlet and outlet, respectively.

$$S_{CO_2} = \frac{n_{CO_2}}{n_{CO,in} - n_{CO,out}} \times 100\% \quad (6)$$

$$S_{Ci} = \frac{i* n_{Ci}}{n_{CO,in} - n_{CO,out}} \times 100\% \quad (7)$$

where C_i represents C1–C5 hydrocarbons, i is the carbon number.

$$S_A = 1 - S_{CO_2} - \sum S_{Ci} \quad (8)$$

where S_A represents selectivity of C attached to aromatic side chain.

In this work, the total carbon molar balance of products and feed was calculated between 93 and 100%. Considering the complexity of the alkylation products of benzene and syngas reaction, the balancing values are reasonable.

3 Results and Discussion

3.1 ^{29}Si MAS NMR

The local environment of Si in the ZSM-5 framework were examined by ^{29}Si solid state MAS NMR. It can be seen that ZSM-5 zeolite has a strong response peak at about − 115 ppm of chemical shift and a small peak located at about − 105 ppm of chemical shift, which represented the group of $Si(OSi)_4$ (denoted as Q4) and $(AlO)Si(OSi)_3$ (denoted as Q3), respectively, as shown in Fig. 1 [25]. Calculated the framework Si/Al of the three ZSM-5 zeolites by formula (1) to be 15, 31, 84, respectively. Since Brønsted acid of ZSM-5 is closely related to framework Al of ZSM-5, this article uses framework Si/Al measured by NMR to link the acidity of zeolite for research.

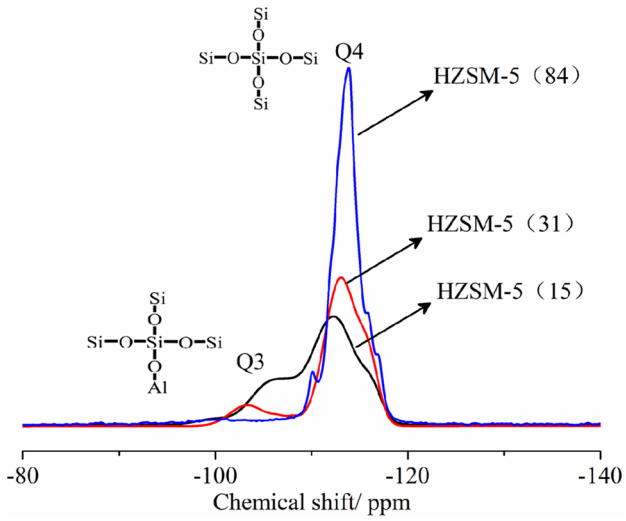

Fig. 1 ^{29}Si MAS NMR spectras patterns of ZSM-5 samples with different Si/Al

3.2 XRD

Figure 2 shows XRD patterns of three fresh hybrid catalysts. The typical characteristic diffraction peaks of MFI (PDF# 44-0003) can be clearly identified in each XRD pattern. The three main characteristic diffraction peaks of CuO and one weak characteristic diffraction peak of ZnO also can be identified in XRD patterns, they corresponding to PDF(#65-2309) and PDF(#65-3411), respectively. There is a sharp characteristic diffraction peak located at 2 theta = 26.4° belongs to graphite (PDF# 01-0646) which are used as adhesive in the CuO–ZnO–Al_2O_3 component [26]. No characteristic diffraction peaks of Al_2O_3 were observed in all XRD patterns, suggesting that Al_2O_3 are highly dispersed in the bifunctional catalysts [27]. XRD spectras of dual-functional catalysts with different mass ratios are shown in Fig. S1. With the increase of the content of CuO–ZnO–Al_2O_3 in the dual function catalyst, the main characteristic diffraction peaks of CuO, ZnO, graphite C become more obvious.

Figure 3 shows XRD patterns of three corresponding used catalysts. The typical characteristic diffraction peaks of MFI, ZnO and C remain, and the peaks of CuO disappear yet, and the peaks of Cu (PDF# 65-9026) appeared clearly. It reveals that CuO was reduced completely by syngas, during the reaction, the metal Cu is considered as the active site for methanol synthesis from syngas [28–30].

3.3 PY-IR

The pyridine adsorbed IR spectra of the ZSM-5 samples at 150 °C were presented in Fig. 4 to differentiate situation

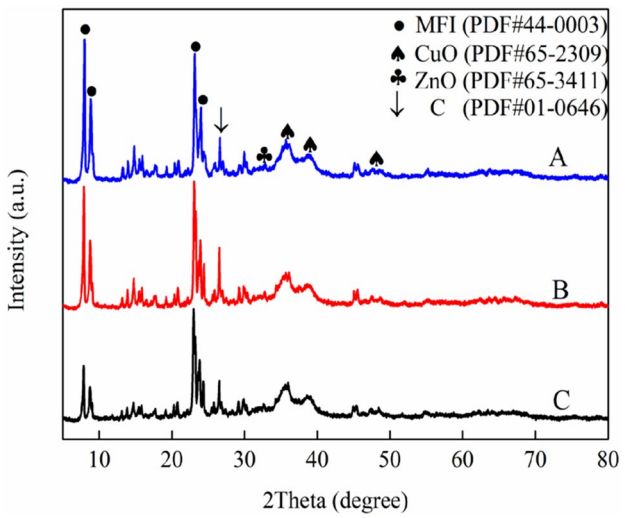

Fig. 2 XRD patterns of fresh CuO–ZnO–Al_2O_3/ZSM-5 samples with different framework Si/Al. **a** CuO–ZnO–Al_2O_3/ZSM-5(84) = 1:1 (mass ratio); **b** CuO–ZnO–Al_2O_3/ZSM-5(31) = 1:1 (mass ratio); **c** CuO–ZnO–Al_2O_3/ZSM-5(15) = 1:1 (mass ratio)

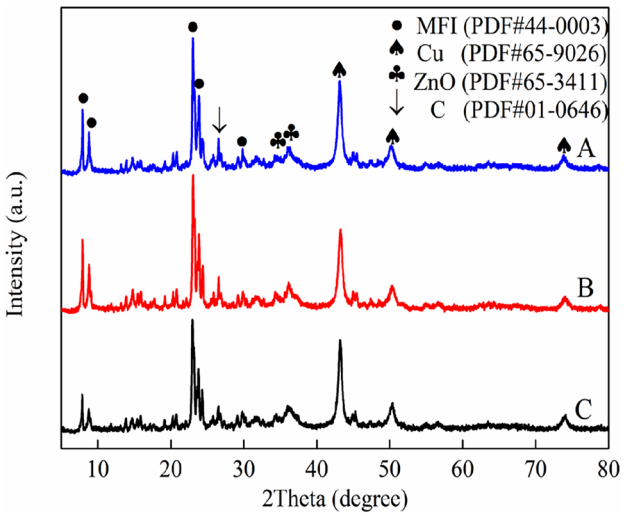

Fig. 3 XRD patterns of used CuO–ZnO–Al_2O_3/ZSM-5 samples with different Si/Al. **a** CuO–ZnO–Al_2O_3/ZSM-5(84) = 1:1 (mass ratio); **b** CuO–ZnO–Al_2O_3/ZSM-5(31) = 1:1 (mass ratio); **c** CuO–ZnO–Al_2O_3/ZSM-5(15) = 1:1 (mass ratio)

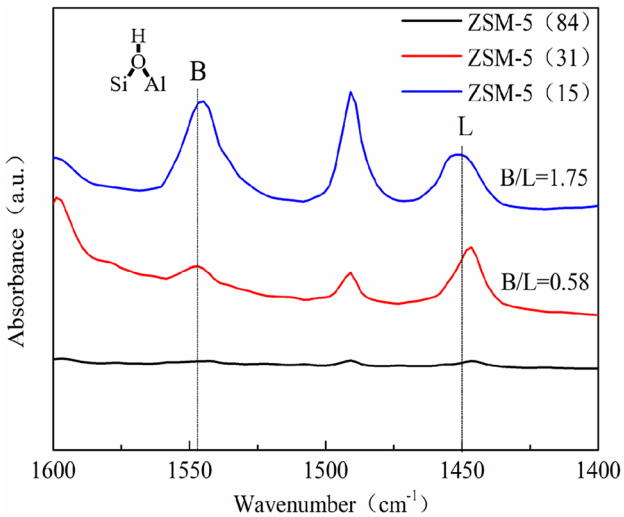

Fig. 4 FT-IR spectra of pyridine adsorption on HZSM-5 with different Si/Al at 150 °C

of Lewis and Brønsted acid sites of ZSM-5. The peaks at 1450 and 1545 cm^{-1} correspond to Lewis acid sites and Brønsted acid sites of ZSM-5, respectively [20, 31, 32]. Brønsted acids mainly come from the -OH group on the framework of ZSM-5 where the Si is replaced by Al, resulting in an imbalance of charge and then -OH produced by adsorption of proton, while Lewis acid mainly originates from the coordinated unsaturated Al^{3+} [33–35]. It can be seen that as the framework Si/Al of ZSM-5 increased from 15 to 84 the peaks referring Brønsted and Lewis acid decreased simultaneously, suggesting that both Brønsted and Lewis acid sites decreased.

3.4 NH_3-TPD

The acidity of ZSM-5 with different Si/Al were detected by NH_3-TPD technology also, as presented in Fig. 5 and the acid amount of the ZSM-5 were summarized in Table 1. Two distinctive desorption peaks at 120–350 °C and above 350 °C were shown for the ZSM-5 (15), which can be attributed to NH_3 desorption from the weak & medium and strong acid sites of zeolite [36–38], respectively. As shown in Table 1, the Si/Al values of the three zeolites measured by XRF are 14, 86 and 140, which is consistent with the law measured by NMR. The difference between the results measured by NMR and XRF due to the presence of non-framework aluminum in the zeolite. It can be seen from the experimental results: as the ratio of Si/Al (NMR and XRF) increases, both desorption peaks became smaller and the peaks position moves to lower temperature, which indicates the acid amount gradually decreases and acid strength has also decreased as Si/Al increases.

3.5 BET and ICP Analysis

The N_2 adsorption desorption isotherms and pore size distribution curves of ZSM-5 and CuO–ZnO–Al_2O_3 were illustrated in Figure S2. All of the ZSM-5 with different Si/Al have a small number of mesoporous pores, which enhance the diffusion of the products and contribute to highactivity. It can be seen from Table 1 and Table S1, the BET surface areas were 311, 371, 400 and 90 m^2/g for ZSM-5(15), ZSM-5(31), ZSM-5(84) and

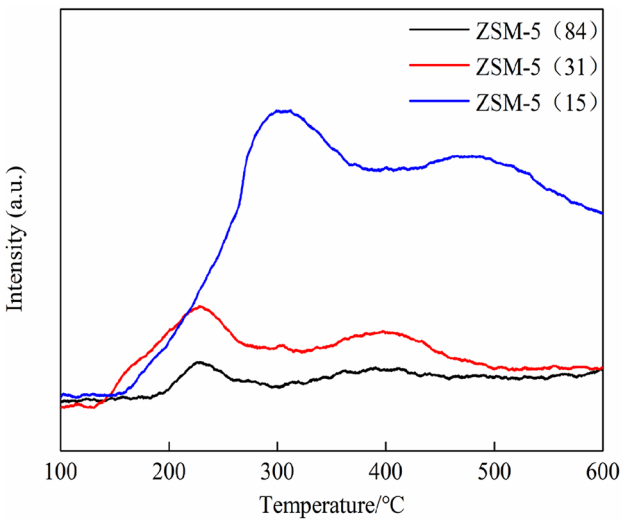

Fig. 5 NH_3-TPD profiles of HZSM-5 with different Si/Al

Table 1 Element composition and texture properties as well as the acidity of HZSM-5 with different Si/Al

Sample (framework Si/Al)[a]	Si/Al[b]	Surface area[c]/ $m^2 \cdot g^{-1}$	Pore volume[c]/ $cm^3 \cdot g^{-1}$	Acid amount (mmol/g)[d]		Total acid amount (mmol/g)[d]
				Weak and Medium	Strong	
HZSM-5[e](15)	14	311	0.22	0.18	0.23	0.41
HZSM-5[e](31)	86	371	0.24	0.06	0.06	0.12
HZSM-5[e](84)	140	400	0.24	0.01	0.02	0.03

[a]Framework Si/Al of ZSM-5 was calculated by formula (1)

[b]Si/Al of ZSM-5 was measured by XRF

[c]Surface area and pore volume were measured by nitrogen adsorption–desorption

[d]Acid amount of ZSM-5 was determined by NH_3-TPD

[e]The residual sodium content of all ZSM-5 is less than 0.6%, measured by ICP

CuO–ZnO–Al_2O_3, with a pore volume of 0.22, 0.24, 0.24 and 0.30 cm^3/g, respectively. With the increase of Si/Al, the surface of zeolites increase correspondingly. In addition, the residual sodium content of ZSM-5 were detected by ICP. The residual sodium content of all ZSM-5 is minimal, indicating that ZSM-5 with different Si/Al are indeed H-type zeolite. The Cu/Zn/Al molar ratio of CuO–ZnO–Al_2O_3 component is 65.8/26.5/7.7, as detected by ICP (Table S1).

3.6 SEM

Figure 6 showed the SEM images of CuO–ZnO–Al_2O_3/ZSM-5(31) bifunctional catalyst and two active ingredients. The ZSM-5 sample has a hexagonal exterior shape with a particle length of around 0.5 μm (Fig. 6a). And the CuO–ZnO–Al_2O_3 (Fig. 6b) showd irregular particles, plates and their aggregates, similar to the morphology observed by Jong-Wook Bae [39], Fang [40], et al. In hybrid catalyst, some of the CuO-ZnO-Al_2O_3 particle clusters are scattered around the ZSM-5 and some of CuO–ZnO–Al_2O_3 particles are deposited on the surface of ZSM-5.

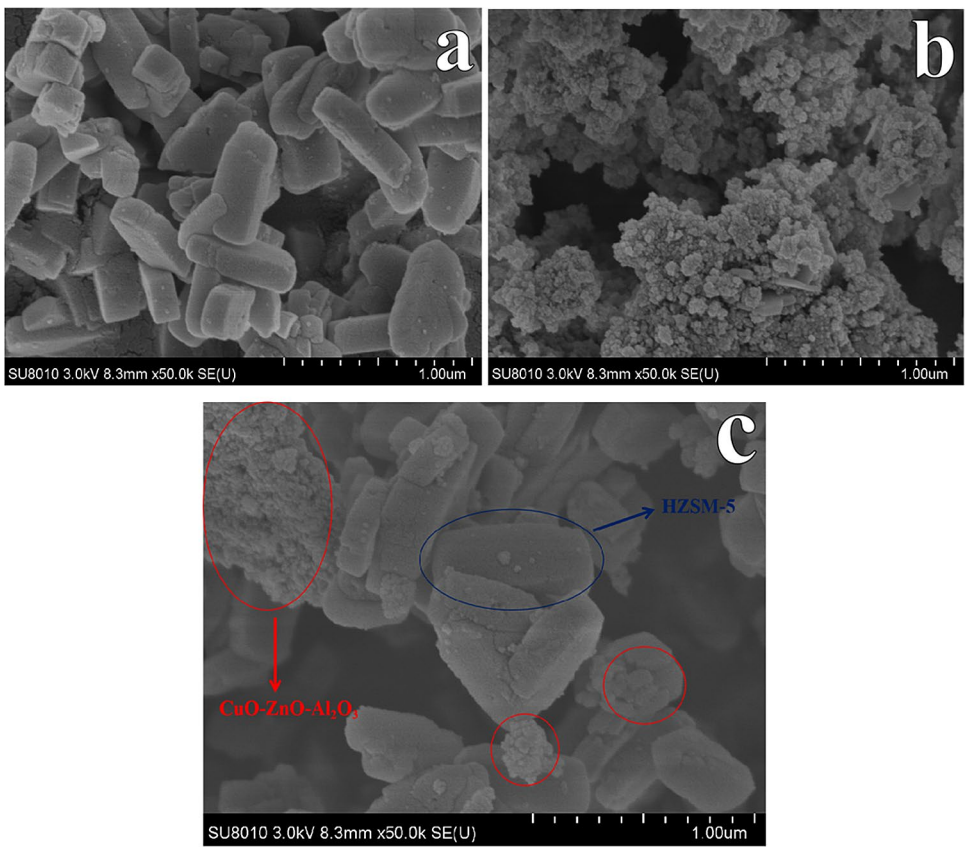

Fig. 6 SEM images of **a** HZSM-531), **b** CuO–ZnO–Al_2O_3 and **c** CuO–ZnO–Al_2O_3/ZSM-5(31) = 1:1 (mass ratio)

3.7 Catalysts Evaluation

3.7.1 Effect of Si/Al on Catalytic Performance

Figure 7 showed the catalytic performance of benzene alkylation with syngas over the Cu–ZnO–Al_2O_3/ZSM-5 with different Si/Al ratios. The benzene conversion of Cu–ZnO–Al_2O_3/ZSM-5(84) was only about 25.2%, while those of Cu–ZnO–Al_2O_3/ZSM-5 with smaller Si/Al showed significant improvements of conversions. The benzene conversion increaseed to 50.7% in Cu–ZnO-Al_2O_3/ZSM-5(31) and then reduced to 45.6% in Cu–ZnO-Al_2O_3/ZSM-5(15). The similar result were found by Yu [19], Gao [41] and Wang [42]. C7 and C8 aromtics, including toluene, ethylbenzene and xylene, are the most important alkylbenzene chemicals. It was observed that for all experiments the total selectivity of C7 and C8 is maintained between 88.7 and 94.4%. It can be seen from Fig. 7 b that the total yield of C7 and C8 of the Cu–ZnO–Al_2O_3/ZSM-5(31) catalyst reached 45.0% which is the highest among all catalysts. For the gaseous phase, CO conversions changes in the same way as benzene conversion, and the Cu–ZnO–Al_2O_3/ZSM-5(31) showed the highest CO conversion of 55.0%. It also showed the highest selectivity of carbon atoms in CO attached to aromatic side chain, suggesting higher efficiency of CO utilization. As for the selectivity of CO_2, CH_4, C2–C5 byproducts, for each catalyst, Cu–ZnO–Al_2O_3/ZSM-5(84) catalyst has higher selectivity of CO_2, which originated from the water–gas-shift reaction [43–45]. And the Cu–ZnO–Al_2O_3/ZSM-5(15) catalyst showed significantly higher C2–C5 selectivity.

The alkylation of benzene and syngas is considered to be the coupling of the two reactions of syngas to methanol and benzene alkylation with methanol. Cu–ZnO–Al_2O_3 and ZSM-5 hybrids can perform relay catalysis, the methanol formed from syngas over Cu–ZnO–Al_2O_3 component undergoes alkylation reaction with benzene at the Brønsted acid sites of the ZSM-5 to produce the target product alkylbenzenes. It was found through detailed experiments carried out at 400 °C, the alkylation of benzene and methanol requires suitable strength and density of Brønsted acids [46].

NMR, PY-IR and NH_3-TPD all showed that Cu–ZnO–Al_2O_3/ZSM-5(31) catalyst contains the appropriate Brønsted acidity, which is the key reason why conversion rate of benzene is the highest and selectivity of C2–C5 byproducts is the lowest. It has been proposed that Brønsted acids played a vital role in the alkylation reaction of benzene and methanol, meanwhile strong Brønsted acids will inevitably catalyze the side reaction of methanol to produce C2–C5 hydrocarbons [47, 48].

Cu–ZnO–Al_2O_3/ZSM-5(15) preferentially catalyzes the side reaction, such as methanol to olefins (MTO) due to its too strong and rich Brønsted acid sites. And the olefins can be hydrogenated to C2–C5 hydrocarbons, or alkylated with

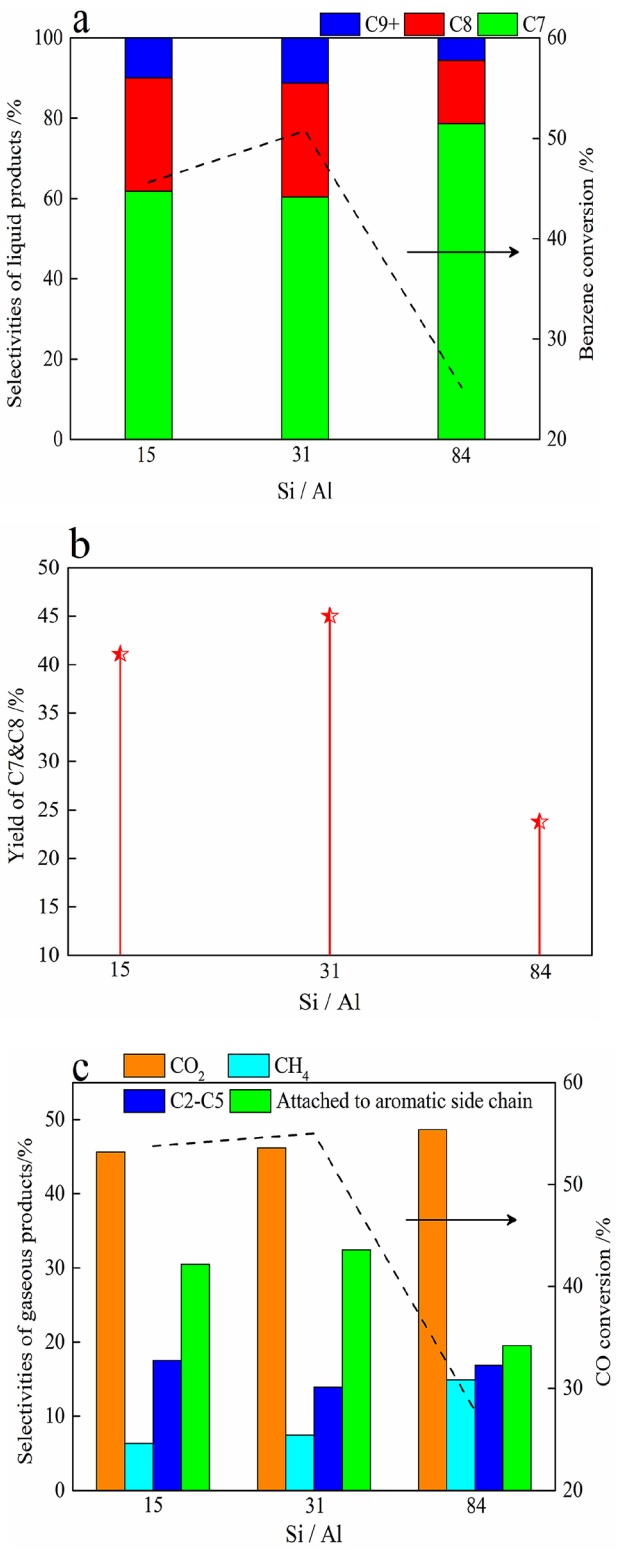

Fig. 7 Effect of Si/Al of ZSM-5 on **a** the liquid products selectivities, **b** the total yield of C7 and C8 and **c** the gas phase products selectivities of Cu–ZnO–Al_2O_3/ZSM-5 catalyst with the mass ratio of two components of 1. Experiment was carried out under 4.0 MPa and 400 °C. Syngas (H_2:CO = 2:1) GHSV = 5220 mL/h g_{cat}. Benzene WHSV = 2.64 g/h g_{cat}

benzene to long-chain alkylated benzenes, thus reduced the amount of methanol directly attached to the aromatic side chain, which leads to a decrease in the conversion of benzene and an increase in the selectivities of ethylbenzene and C2–C5. The increase in ethylbenzene leads to a decrease in the selectivity of para-xylene in C8, which is the most demanded of alkylbenzenes. When the Si/Al of the dual-function catalyst increases to 84, too weak Brønsted acid will limit the alkylation reaction, which leads to the syngas to be converted into CH_4, CO_2, C2–C5 under the catalysis of Cu–ZnO–Al_2O_3. This is due to that if the methanol cannot be consumed by the alkylation immediately the syngas will be favored to produce more byproducts, such as CO_2 and hydrocarbons, especially at high temperature. By constructing the relationship between the catalyst acid density and the activity (Table S2), it was found that the appropriate increase of the catalyst acid density was conducive to the rapid alkylation of methanol intermediates and benzene, improving the activity, but too high acid density would give priority to the conversion of methanol into hydrocarbons, leading to the decrease of the alkylation activity.

Based on above discussion, it was reasonable to conclude that the catalyst with appropriate Brønsted acid strength and acid density can exhibit the highest activity due to minimize the occurrence of the side reaction of methanol.

3.7.2 Effect of Reaction Temperature on Catalytic Performance

Figure 8 showed the catalytic performance of Cu–ZnO–Al_2O_3/ZSM-5(31) catalyst in the alkylation of benzene with syngas at different reaction temperatures. As the reaction temperature increased from 300 to 450 °C, the conversion of benzene showed an increase from 23.9 to 50.7% at 400 °C, and then dropped to 39.5% at 450 °C, the conversion of benzene reached the highest maximum at 400 °C. The change trend of the total yield of C7 and C8 is consistent with that of the benzene conversion, reaching the maximum of 45.0% at 400 °C. As shown in Fig S3, when the reaction temperature is 400 °C, the CO conversion rate is the highest and the selectivity of CO participating in the alkylation reaction is also the highest. No methanol intermediate were detected in product, except at 300 °C, 0.5% of methanol was detected in the liquid phase product, suggesting that the methanol was consumed immediately by alkylation of benzene at higher reaction temperature.

There is a temperature matching relationship between the two components in the Cu–ZnO–Al_2O_3/ZSM-5(31) dual-function catalyst [20, 49]. Generally, the temperature of Cu–ZnO–Al_2O_3 catalyzed synthesis of methanol at 230–280 °C [50–52], while the HZSM-5 catalyzed benzene and methanol alkylation needs to be higher than 400 °C [20, 49]. In the Cu–ZnO–Al_2O_3/ZSM-5(31) catalyzed alkylation

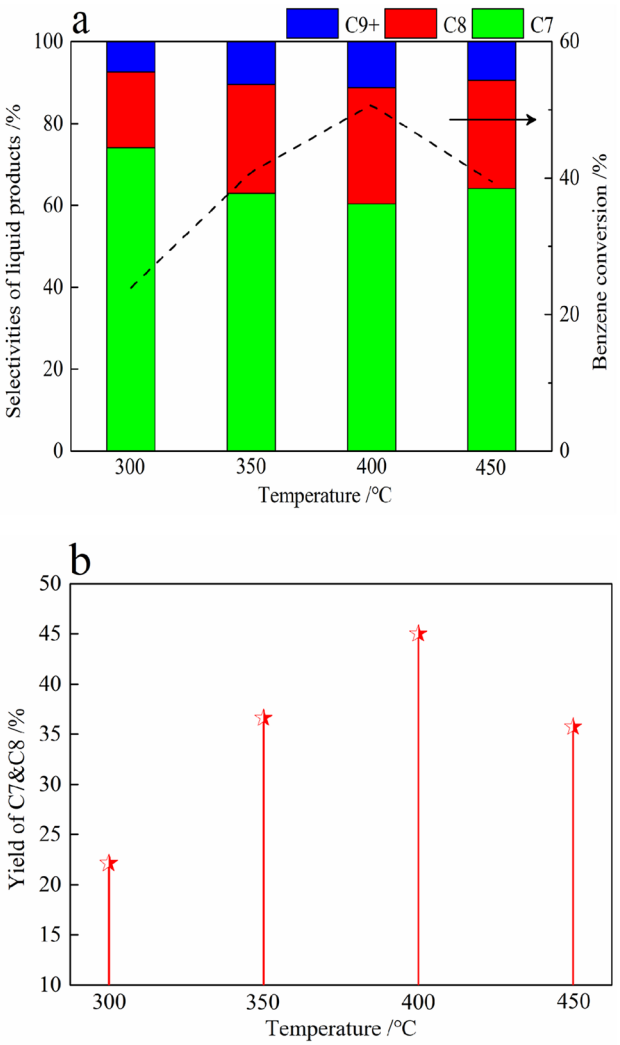

Fig. 8 Effect of reaction temperature on **a** the liquid products selectivities and **b** the total yield of C7 and C8 of Cu–ZnO–Al_2O_3/ZSM-5(31) catalyst with the mass ratio of two component of 1. All experiment was carried out under 4.0 MPa. Syngas (H_2:CO = 2:1) GHSV = 5220 mL/h g_{cat}. Benzene WHSV = 2.64 g/h g_{cat}

reaction of benzene and syngas, when the temperature is lower than 400 °C, although it is beneficial to the production of intermediate methanol from syngas on Cu–ZnO–Al_2O_3, the ability of ZSM-5 to activate benzene is limited due to the low reaction temperature. Therefore, when the reaction temperature is lower than 400 °C, the benzene alkylation rate is low and the selectivity of by-products increase. As an active phase of high temperature methanol synthesis, ZnO component has a synergistic effect with Cu at over 400 °C to produce methanol [52, 53]. In addition, the generated methanol will be continuously consumed by the alkylation reaction, breaking the thermodynamic balance of methanol synthesis, resulting in an increase in the methanol synthesis capacity of Cu–ZnO–Al_2O_3 at high temperatures. Thus the

coupling reaction reached its maxium activity at 400 °C. In addition, due to the optimal coordination of the two-stage reaction at this temperature, the maximum alkylation utilization rate of CO is achieved. But when the temperature reaches 450 °C, the excessively high reaction temperature caused the Cu to sinter quickly, suppressing the synthesis of methanol. Without the sufficient methanol produced, and the catalyst activity was decreased.

Therefore, the optimal reaction temperature of Cu–ZnO–Al_2O_3/ZSM-5(31) catalyzed benzene and syngas alkylation is 400 °C. At this temperature, the two active components of bifunctional catalysts can exploit their respective advantages to the full and achieve the best catalytic effect.

3.7.3 Effect of Mass Ratio of Cu–ZnO-Al_2O_3 and ZSM-5 on Catalytic Performance

The effects of different mass ratios of Cu–ZnO–Al_2O_3 and ZSM-5 on the catalytic performance of dual-function catalysts can be seen in Fig. 9. When there was only Cu–ZnO–Al_2O_3 component, the benzene conversion rate is only 14.2%, and there is only a small amount of toluene in the product, no C7 + product is detected. At the same time, there are 10.7% cyclohexane in the liquid phase product. So it is reasonable that pure Cu–ZnO–Al_2O_3 is hardly active to catalyzing the alkylation reaction of benzene, and preferentially catalyzes the hydrogenation reaction of benzene; When the catalyst only contain ZSM-5 component, benzene does not react, the CO conversion rate is only 2.0%, and the main gas phase product is CH_4, this result is similar to Fan's[49]. The specific gas phase product distribution is shown in Fig. S4, the CO conversion rate reaches the maximum when the mass ratio of the two components is 1. As the mass ratio of Cu–ZnO–Al_2O_3/ZSM-5 gradually decreases from 5:1 to 1:5, the conversion rate of benzene and the total yield of C7&C8 are volcano curves, namely first increases and then decreases. When the mass ratio of the two components is 1:1, activity and yield reach their maximum values simultaneously.

The two active components of Cu–ZnO–Al_2O_3 and ZSM-5 in the dual-function catalyst perform relay catalysis. In the first step, Cu–ZnO–Al_2O_3 catalyzed synthesis of methanol, and then ZSM-5 catalyzed the alkylation of benzene and methanol to alkylbenzenes in the second step. The most suitable ratio of Cu–ZnO–Al_2O_3 with ZSM-5 can generate an appropriate amount of methanol intermediates to react with benzene, minimize side reactions of methanol. In addition, the proper amount of ZSM-5 can rapidly catalyze the alkylation reaction of methanol and benzene at an appropriate temperature, breaking the thermodynamic equilibrium of methanol synthesis, and making the entire reaction system proceed in the direction required. When the proportion of Cu–ZnO–Al_2O_3 in the bifunctional catalyst is too high, more methanol intermediates will be generated. On the contrary, the less ZSM-5 leads to insufficient catalytic alkylation, formed methanol cannot be alkylated, or be converted into by-products. Similarly, when the proportion of Cu–ZnO–Al_2O_3 is too small, too few methanol intermediates are produced, which limits the alkylation of benzene and methanol. Therefore, when the two active components of Cu–ZnO-Al_2O_3/ZSM-5 are mechanically mixed with the mass ratio of 1:1, the catalytic effect of benzene and syngas is the optimal.

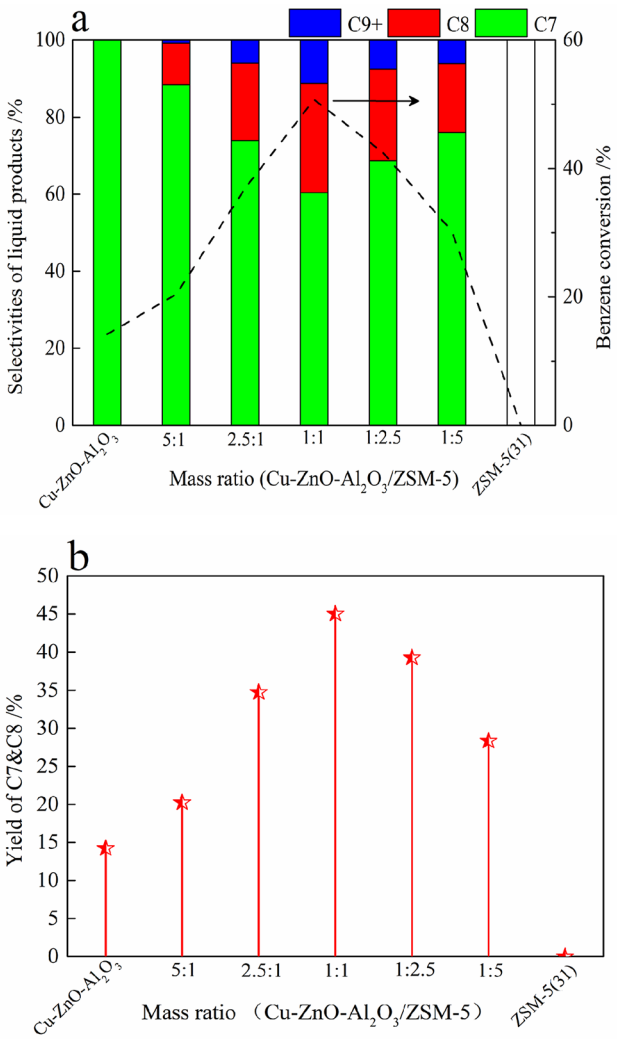

Fig. 9 Effect of mass ratio of Cu–ZnO–Al_2O_3 and ZSM-5 on **a** the liquid products selectivities and **b** the total yield of C7 and C8 of Cu–ZnO–Al_2O_3/ZSM-5(31) catalysts. All experiment was carried out under 400 °C, 4.0 MPa. Syngas (H_2:CO = 2:1) GHSV = 5220 mL/h g_{cat}. Benzene WHSV = 2.64 g/h g_{cat}

3.8 Stability Tests

The 24 h stability tests of Cu–ZnO–Al_2O_3/ZSM-5 is shown in Fig. 10. It can be seen from the Fig. 10 that the initial

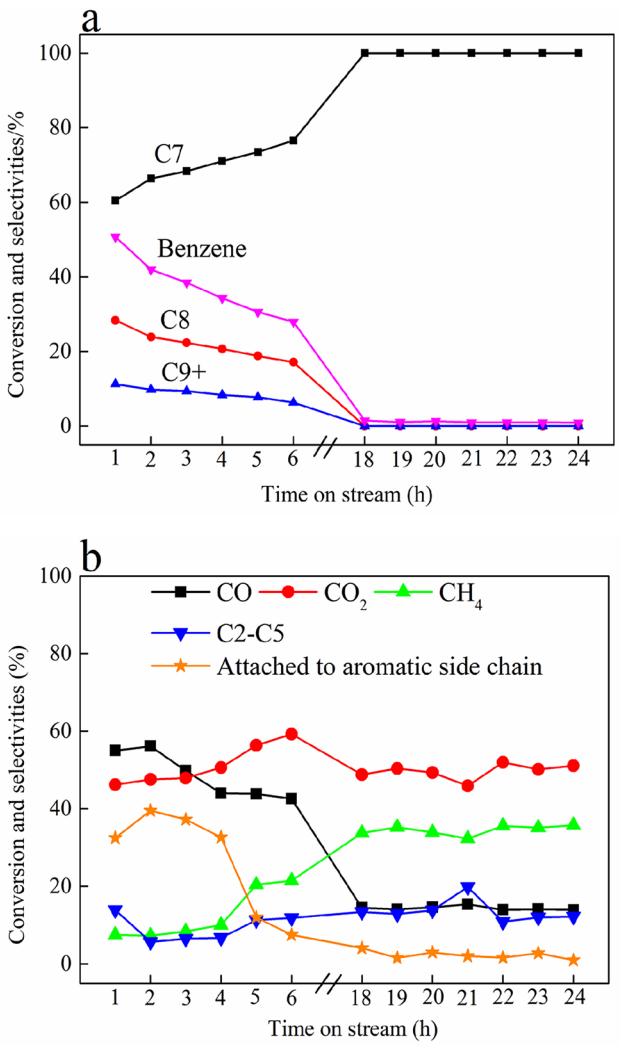

Fig. 10 Stability of Cu–ZnO–Al_2O_3/ZSM-5(31) in alkylation of benzene with syngas. All experiment was carried out under 400 °C, 4.0 MPa. Syngas (H_2:CO = 2:1) GHSV = 5220 mL/h g_{cat}. Benzene WHSV = 2.64 g/h g_{cat}

conversion rate of benzene and CO is the highest. But as the reaction runs, the conversion rate drops rapidly, and the catalyst is deactivated after the reaction runs stably for 18 h.

The experimental results show that the Cu–ZnO–Al_2O_3/ZSM-5 has a high initial conversion rate, which illustrates that Cu–ZnO–Al_2O_3 component has a strong ability to catalyze methanol synthesis, even at relatively high temperatures. However, Cu is easy to sinter at high temperature, the high reaction temperature causes the methanol synthesis capacity of hybrid catalyst to decrease with time [22]. In addition, as the reaction progresses, carbon deposition on zeolite is also an important cause of catalyst deactivation [54]. The studies of Kang [55], Zhou [56] and Zhang [57] have shown that the coordination of various components in the catalyst in the tandem reaction is an important reason for achieving excellent catalytic effects. Therefore, the hybrid catalyst will further improves the reaction activity,selectivity and stability through the optimal matching of the two components in the future.

3.9 Reaction Pathway and Mechanism

The alkylation of benzene and syngas is a very complex reaction system, which involves multiple reactions occurring simultaneously. By studying the effect of Si/Al of ZSM-5 on the catalytic performance, it is found that when the Brønsted acidity of zeolite is too weak, the benzene conversion rate decreases while the gas by-products increase. When the zeolite has too strong Brønsted acidity, the side reaction of methanol intermediate increase. Therefore, we infered the reaction paths of catalysts with different acid properties based on the product distribution and showed in Fig. 11.

Firstly, Cu–ZnO–Al_2O_3 catalyzes the syngas to generate methanol, then the methanol moves to Brønsted acid sites of the zeolite and reacts with benzene to generate toluene, the alkylated benzene can reacts secondly to produce xylene and C9+ aromatics. It is worth noting that the role of ZnO and Al_2O_3 in the alkylation reaction of benzene and syngas is very important, ZnO alone has the ability to synthesize methanol [58] and can produce a synergistic effect with Cu, moreover Al_2O_3 is often used as an additive to increase the surface area of the catalyst and improve the catalyst active [30, 59–61].

Simultaneously, the methanol intermediate produced is prone to many reactions such as MTO [62]., MTG [63, 64] and MTA [65] on the acid sites of the zeolite. As shown in Table S3, very high alkanes content, due to (1) reactions such as MTG and MTA occur on the acid sites of zeolite, (2) olefin hydrogenation reaction on Cu–ZnO–Al_2O_3 surface. The zeolite has too weak Brønsted acid sites, methanol cannot be consumed in time through the alkylation reaction, which causes the syngas to generate CH_4, C2–C5, CO_2 under the catalysis of Cu–ZnO–Al_2O_3, as evidenced by the reaction on pure Cu–ZnO–Al_2O_3 (Fig. S4). CO_2 in gas phase productsis considered to be mainly formed by the water gas shift reaction [66, 67]. Based on the above discussion, we proposed the reaction paths on hybrid catalysts with different acidity, as shown in Fig. 11. When the Si/Al of ZSM-5 is smaller and ZSM-5 contains more strong Brønsted acid, the entire reaction system will be biased towards the reaction path 1, the content of toluene and xylene will decrease while ethylbenzene, cumene, CH_4, and C2-C5 content will increase due to mainly the side reaction of methanol; When the Si/Al of ZSM-5 is suitable, the entire reaction system will be proceed towards the reaction path 2, and more toluene and xylene alkylated products will be generated; when the Si/Al of ZSM-5 is large, the Brønsted acid of ZSM-5 is too weak, the entire reaction system will be biased towards

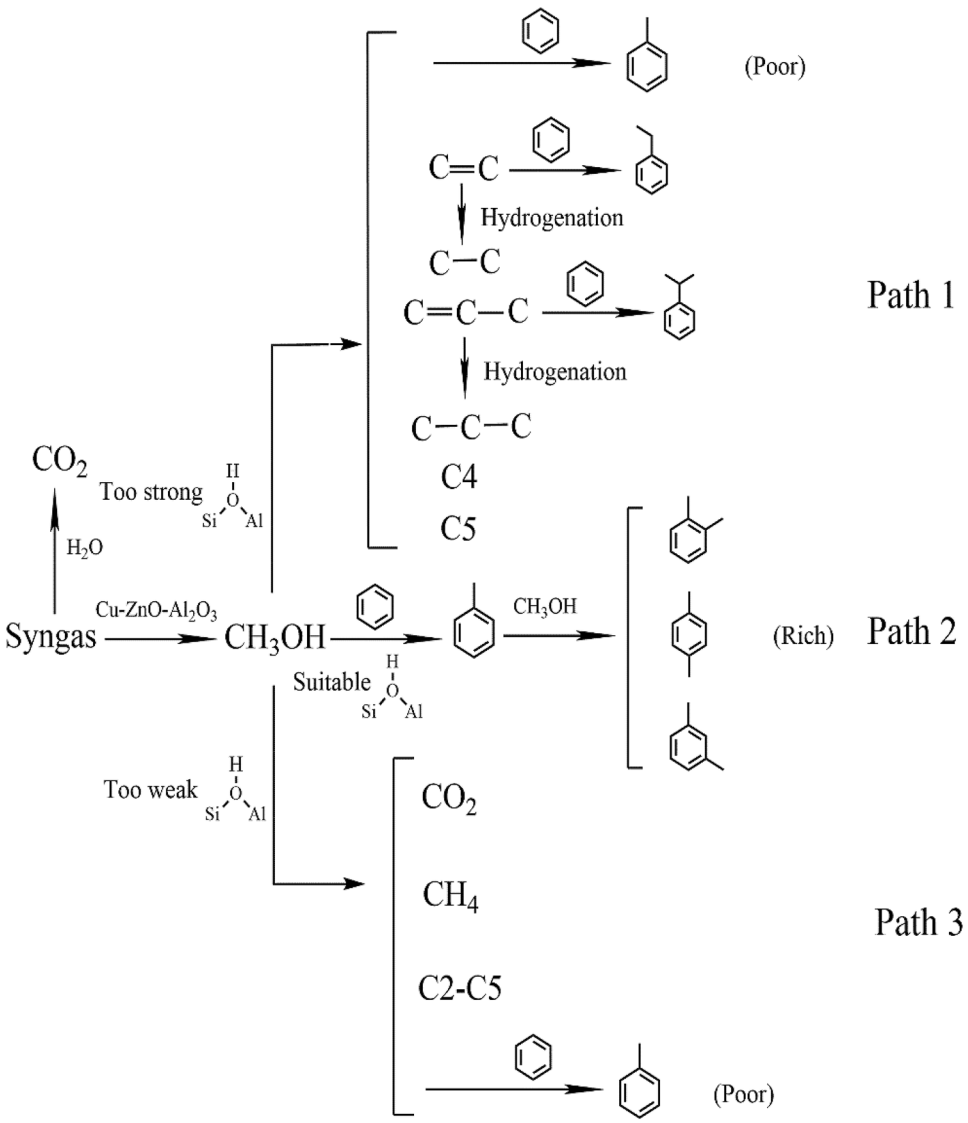

Fig. 11 The reaction paths over different active sits in the benzene alkylation with syngas

the reaction path 3, generating less toluene and more CO_4, CO_2, C2-C5. Therefore, we can control the acidity of the zeolite in the dual-function catalyst to achieve different reaction paths according to product requirements.

4 Conclusion

A high-activity dual-functional Cu–ZnO–Al_2O_3/ZSM-5 catalyst is developed for the alkylation of benzene with syngas. The catalyst realizes the one-step manufacture of alkylbenzenes from benzene and syngas through the coordination of two active components and methanol is deemed as the reaction intermediate. By studying the influence of Si/Al on the catalytic performance, we found that the Brønsted acid acid of the dual-functional catalyst is indispensable for alkylation of benzene, but too much strong Brønsted acid will preferentially convert methanol intermediate to hydrocarbons, resulting in a decrease of activity, and the optimal framework Si/Al is 31.

According to the product distribution, the reaction paths are inferred. Among them, ethylbenzene and cumene mainly come from the alkylation of benzene with ethylene and propylene which are produced by the MTO, CO_2 mainly comes from the water gas shift reaction, and CH_4, C2–C5 mainly come from the side reaction of methanol intermediates.

Benzene conversion of 50.7%, CO conversion of 55.0% and total yield to C7 and C8 of 45.0% are achieved over Cu–ZnO–Al_2O_3/ZSM-5(31) = 1:1 (mass ratio) at 400 °C and 4 MPa. Our optimal catalyst can make the two active components of the dual function catalyst achieve a better match, achieve higher activity.

Supplementary Information The online version contains supplementary material available at https://doi.org/10.1007/s10562-021-03617-5.

Acknowledgements This project was sponsored financially by the National Natural Science Foundation of China (No. 22078351)

Declarations

Conflict of interest The all authors declare that they have no conflict of interest.

References

1. Kocal JA, Vora BV, Imai T (2001) Appl Catal A Gen 221:295–301
2. Zhang H, Cheng YT, Vispute TP, XiaoG R, Huber W (2011) Energy Environ Sci 4:2297
3. Goursaud S, MombrunD M, Cheyron D (2020) ERJ Open Res 6:00182–02020
4. ER Graef, JW Liew, AH Kim, JA Sparks (2020) Ann Rheum Dis Annrheum 1-2
5. Cheng K, Zhou W, Kang J, He S, Shi S, Zhang Q, Pan Y, Wen W, Wang Y (2017) Chemistry 3:334–347
6. Zhang P, Tan L, Yang G, Tsubaki N (2017) Chem Sci 8:7941–7946
7. Arslan MT, Qureshi BA, Gilani SZA, Cai D, Ma Y, Usman M, Chen X, Wang Y, Wei F (2019) ACS Catal. 9:2203–2212
8. Xu Y, Liu J, Wang J, Ma G, Lin J, Yang Y, Li Y, Zhang C, Ding M (2019) ACS Catal 9:5147–5156
9. Ni Y, Sun A, Wu X, Hai G, Hu J, Tao L, Li G (2011) Micropor Mesopor Mater 143:435–442
10. Zhang J, Qian W, Kong C, Fei W (2015) ACS Catal 5:2982–2988
11. Rakoczy J, Romotowski T (1993) Zeolites 13:256–260
12. Gao K, Li S, Wang L, Wang W (2015) RSC Adv 5:45098–45105
13. Dong P, Li Z, Wang D, Wang X, Guo Y, Li G, Zhang D (2018) Catal Lett 149:1
14. Guixian L, Guo Y, Liu J, Dong JI, Wang D, Yang Y, Zhang Y, Chao WU (2019) Chem Ind Eng Prog 12:8
15. Zhong J, Liu X, Zhu XD (2016) Petroleum Refining and Chemical Industry 47:62–66
16. Bai Y, Yang F, Liu X, Liu C, Zhu X (2018) Catal Lett 148:3618–3627
17. Fan Y, Jie Z, Liu X, Zhu X (2018) Appl Energy 226:22–30
18. Pang WW, Gu HH (2018) Nat Gas Chem Ind 43:67–71
19. Yu B, Ding CM, Liu P (2019) Nat Gas Chem Ind 44:24–29
20. Yu B, Ding C, Wang J, Zhang Y, Meng Y, Dong J, Ge H, Li X (2019) J Phys Chem C 123:18993–19004
21. Gao B, Ding C, Wang J, Ding G, Dong J, Ge H, Li X (2020) New J Chem 44:2471–2478
22. Zhao X, Zeng F, Zhao B, Gu H (2015) China Pet Process Petrochem Technol 17:31–38
23. Gao B, Ding C, Wang J, Ding G, Dong J, Ge H, Li X (2020) New J Chem 44:1
24. Hartanto D, Yuan LS, Sari SM, Sugiarso D, Nur H (2016) J Teknol 78:223–228
25. Hu SF, Wang Y, Ma JH, Li RF (2019) J Inorg Chem 35:2253–2259
26. Chu Z, Chen H, Yu Y, Wang Q, Fang D (2013) J Mol Catal A Chem 366:48–53
27. Bahmani M, Farahani BV, Sahebdelfar S (2016) Appl Catal A 520:178–187
28. Chinchen GC, Denny PJ, Jennings JR, Spencer MS, Waugh KC (1988) ChemInform 19:1–65
29. Hadden RA, Sakakini B, Tabatabaei J (1997) Catal Lett 44:145–151
30. Sun JT, Metcalfe IS, Sahibzada M (1999) Ind Eng Chem Res 38:3868–3872
31. Song YQ, Feng YL, Liu F, Kang CL, Zhou XL, XuG LY, Yu X (2009) J Mol Catal A Chem 310:130–137
32. Wei R, Li C, Yang C, Shan H (2011) J Nat Gas Chem 20:261–265
33. Marturano P, Drozdová L, Kogelbauer A, Prins R (2000) J Catal 192:236–247
34. Dedecek J, Sklenak S, Li C, Wichterlova B, Sauer J (2009) J Phys Chem C 113:14454–14466
35. Liu J, Zhang H, Lu N, Yan X, Li R (2020) Ind Eng Chem Res 59:1056–1064
36. Narayanan S, Sultana A, Le QT, Auroux A (1998) Appl Catal A 168:373–384
37. Jiang F, Zeng L, Li S, Liu G, Wang S, Gong J (2015) ACS Catal 5:438–447
38. Zhou W, Zhao Y, Wang Y, Wang P, Shengping X, Ma P, Xinbin X (2016) ChemCatChem 8:3663–3671
39. Bae JW, Potdar HS, Kang S, Jun K (2008) Energy Fuels 22:223–230
40. Zhang F, Zhang Y, Yuan L, Gasem KAM, Chen J, Chiang F, Wang Y, Fan M (2017) Mol Catal 441:190–198
41. Gao BZ, Ding CM, Ding GY (2020) Nat Gas Chem Ind 45:22–44
42. Wang Q, Cen J, Lyu J, Li X, Zhang Q (2016) Catal Sci Technol 6:2647–2652
43. Sun Y, Hla SS, Duffy GJ, Cousins AJ, French D, Morpeth LD, EdwardsD JH, Roberts G (2011) Catal Commun 12:304–309
44. Studt F, Behrens M (2015) ChemCatChem 7:7
45. Kondrat S, Smith P, Carter J, Hayward J, Pudge G, Shaw G, Spencer M, Bartley JK, Taylor SH, Hutchings G (2016) Faraday Discuss 10:1039
46. Adebajo MO, HoweM RF, Long A (2000) Catal Today 63:471–478
47. Hu H, Zhang Q, Cen J, Li X (2014) Catal Commun 57:129–133
48. Hu H, Lyu J, Cen J, Zhang Q, Wang Q, Han W, Rui J, Li X (2015) RSC Adv 5:63044–63049
49. Yang F, Fang Y, Liu X, Liu X, Muir D, Maclennan A, Zhu X (2019) Ind Eng Chem Res 58:13879–13888
50. Choi Y, Stenger HG (2002) Appl Catal B 38:259–269
51. Behrens M, Studt F, Kasatkin I, Kuhl S, Havecker M, Abildpedersen F, Zander S, Girgsdies F, Kurr P, Kniep B (2012) Science 336:893–897
52. Li D, Xu S, Cai Y, Chen C, Zhan Y, Jiang L (2017) Ind Eng Chem Res 56:3175–3183
53. Sun J, Wan S, Wang F, Lin J, Wang Y (2015) Ind Eng Chem Res 54:150717–170237007
54. Liu J, Chen W, Wang Q, Xu L (1999) J Thermal Anal Calorimet 58:375–381
55. Kang J, He S, Zhou W, Shen Z, Li Y, Chen M, Zhang Q, Wang Y (2020) Nat Commun 11:827
56. Zhou B, Wang H, Cao ZY, Zhu JW, Jia YX (2020) Nat Commun 11:1–10
57. Zhang P, Tan L, Yang G, Tsubaki N (2017) Chem Sci 10:1039J
58. Youming N, Zhiyang C, Yi F, Yong L, Wenliang Z, Zhongmin L (2018) Nat Commun 9:3457
59. Bart JCJ, Sneeden RPA (1987) Catal Today 2:1–124
60. Chen HY, Chen L, Lin J, Tan KL, Li J (1998) J Phys Chem B 102:1994–2000
61. Shishido T, Yamamoto Y, Morioka H, Takaki K, Takehira K (2004) Appl Catal A 263:249–253
62. Adebajo MO, Long MA (2003) Catal Commun 4:71–76

63. BjRgen M, Joensen F, Holm MS, Olsbye U, Lillerud KP, Svelle S (2008) Appl Catal A 345:43–50
64. Benito PL, Gayubo AG, Aguayo AT, Olazar M, Bilbao J (2015) J Chem Technol Biotechnol 66:183–191
65. Conte M, Lopez-Sanchez JA, Qian H, Morgan DJ, Hutchings GJ (2011) Catal Sci Technol 2:105–112
66. Li Y, Fu Q, Flytzani-Stephanopoulos M (2000) Appl Catal B Environ 27:179–191
67. Bahmani M, Vasheghani Farahani B, Sahebdelfar S (2016) Appl Catal A 520:178–187